Spectral analysis of an AVIRIS image of San Pedro Channel

Curtiss O. Davis, Mike 1 Iamilton, W. Joe Rhea and Jeannette van den Bosch

Jet Propulsion 1 aboratory
California Institute of Technology
4800 Oak Grove Dr., Pasadena, CA 91109

Kendal 1 Carder and Robert Steward

University of South Florida
1 Department of Marine, Science
140 Seventh Ave.. S., St. Petersburg, FL 33701

Abstract

Optical case-2 waters near an ocean outfall were examined, using a combination of AVIRIS imagery and ship-based surface and profile bio-optical measurements. IIio-optics] mooring data were useful in determining, the hydrodynamics of the area. After correcting the image to units of water-leaving radiance (1_w), excellent agreement was achieved between remotely-sensed and in-situ measurements. Spectra from visibly different areas were extracted and compared to the in-water measurements and to each other. NeaI-shore spectra were dominated by the presence of suspended sediment from beach erosion. Spectra from the central part of the image had a characteristic signature from particulates from either the outfall 01 resuspension of bottom material or both. At the offshore. edge. of the image. elevated levels of chlorophyll had the greatest influence on spectral shape. Backscatter at 660 nm was calculated from the AVIRIS data and a backscatter image was produced which clearly showed the. distribution of the two types of sediments.

There was a large swell at the time. of the over flight and the side of the swell towards the sun was significantly brighter due to surface reflected sunlight. The light and dark pattern was examined in detail, and the difference between the light and dark portions of the image was quantified. A moderate resolution imager such as SeaWiFS would average the. light and dark pixels, and retrieve a falsely high water leaving radiance signal.

1. Introduction

Approximately 374 million gallons of treated wastewater per day from Los Angeles County are introduced into the coastal ocean near White Point, on the Pales Verdes Peninsula. The effluent is discharged through two diffusers, and mixes with the surrounding watt.rs at a rate determined in parl by local physical processes. Normally the plant adequately treats the sewage, however, 1 .os Angeles has combined storm drains and sewers and during stormy periods in the winter the flow exceeds the plants capacity and a combination of street runoff and partially treated sewage is released into the ocean. Beach closings in the vicinity of this and other Southern California se.wage outfalls are common following storm events. An additional concern is that during these energetic periods, previously deposited sediments may be resuspended and mixed up into the water column releasing DDT and other toxic materials that were discharged into the. ocean in the 1940s anti 1950s.

Previous studies near the, outfall have focused on transport and dispersion of the plume[1-4]. in addition, Wu et al.[2] and Washburn et al.[4] have described the. resuspension of bottom sediments during periods of increased currents and have elucidated techniques for separating the particle signal into photosynthetic and non photosynthetic components, using bio-optical measurements. in this study we use aircraft remote. sensing ocean color measurements validated with in situ measurements to dcline.ate, the extent of the plum and dc.scribe other features in the San Pedro Channel.

"1"0 date ocean color remote sensing has focused primarily on mesoscale and ocean basi n scale feat roes, For example the Se,a-Viewing Wide Field of View Sensor (SeaWiFS)[5] will be launched early next year and will provide global data at 4.5 km resolution and regional data at 1.13 km resolution in 8 selected bands. This will be an excellent data set for many oceanic problems, and it is expected to be used by a large community of oceanographers for research and an even broader group for some commercial applicat ions. 1 lowever, there are many circumstances where SeaWiFS will not provide. useful data, such as in the near coastal areas which require higher spatial resolution and in case 2 waters[6] where dissolved organics, suspended sediments and bottom reflection can interfere with the chlorophyll signal. 1 n addition, SeaWiFS is highly tuned for ocean applications and it saturates over most land scenes, and over clouds. This means that if the scan is from the land to the ocean then the instrument is still 'ringing' from the. saturation and the. ocean data is not usable for up to 10 pixels, or 11 km from the shore. For many coastal ocean sites this is a huge loss. For example, ringing will mean that the SeaWiFS data for San Francisco Bay is essentially all contaminated, as it is on average only 10 km wide.. Also, estuaries have high sediment and dissolved organics and the. SeaWiFS band set is inadequate to resolve the chlorophyll signal from these, competing, signals. Other areas that will provide difficulties for SeaWiFS are the. Mississippi River Plume and other river plume.s which have high sediment loads.

To overcome these problems wc have been using the Airborne Visible/Infrared Imaging Spectrometer (AVIRIS)[7] m study coastal ecosystems. AVIRIS has 10 nm spectral anti 20 m spatial resolution and preliminary algorithms have been developed for case 2 waters[8,9]. There is no ringing evident in AVIRIS data as AVIRIS has sufficient dynamic range to handle cloud, land and ocean scenes. With 20 m spatial resolution it is possible to image even the smallest bays and estuaries. Here we use AVIRIS data to study coastal erosion and the plume from a large sewage outfall.

2. Study site and AVIRIS data collection

AVIRIS images of the White Point/San Pedro Channel area (figure 1) and supporting ship data were acquired on March 21, 1991. Several storms had passed through the area in the weeks preceding the. experiment and 20 knot winds and a large swell persisted on the. day of sampling. During AVIRIS data collection, the solar zenith angle was 36.5° and the azimuthal angle was 2.05.6°. 'l'he flight line was directly away from the sun to minimize sunglint anti uneven illumination. A total of ten ocean scenes were collected, covering the San Pedro Channel between the l'ales Verdes Peninsula and Catalina Island, in two swaths. Each AVIRIS scene is 10 by 12 kilometers with 20 m spatial resolution. The data are stored as a spectral data cube; 614 samples by 512 lines by 2.20 spectral bands. The spectral coverage of the instrument is from ().4 to 2.4 μm, anti each channel has an approximately Gaussian response with a nominal 10 nm width at half maximum signal.

AVIRIS was originally designed to study land tar gets and the signal-to- noise performance was marginal for- dark targets such as the ocean [10] In response to the need for improved signal to noise in the visible the AVIRIS team has made many improvements in AVIRIS performance. This data, collected in early 1991, was free of patterned noise and we obtained good average spectra binning 5x5 pixels, which resulted in 100 m spatial resolution.

A few clouds can be seen in the images, but overall visibility was quite good. For this analysis, the. two images closest to White Point were concatenated, for a total of614 lines of image data. The combined image was spectrally subsampled, and only the spectral range 0.4 to 1.2 pm was analyzed.

3. *In-situ* measurements

At the. time of the overflight optical profile data WCJC acquired using a Bio-Optical Profiling System (BOPS)[11]. The BOPS is based on a Biospherical Instruments (San Diego, CA) MER 1048 which measures spectra] downwelling irradiance and upwelling irradiance and radiance (including 683 nm fluorescence), photosynthetically available radiation (l'AR), depth, tilt and roll. Temperature and salinity

were measured with a SeaBird CTD, chloroph y]] with a Sea Tech fluorometer and beam transmission (660 nm) with a Sea Tech transmissometer. Simultaneously surface, downwelling irradiance was collected with a four channel deck cell. The BOPS data were binned to 1 m depth intervals and processed to remove, ship reflection or shadow and other possible. artifacts using interactive software which we dcve.loped for this purpose using the Interactive Data Language (IDL, Research Systems, inc.).

Measurements of remote-sensing reflectance of the sea surface, (R_{rs}), from 350 to 1250 nm were made. with a Spectron Engineering Model 590 handheld spectroradiometer following the procedures of Hamilton, et al. [12] and references cited therein. Sea surface reflectance was measured relative to a gray 10% reflectance standard and corrections were made for reflected skylight, Because of the. rough sea state and abundance of foam at station 1, only the. Rrs spectrum from station ? was used in this analysis.

Water samples were, collected at four depths for determination of chlorophyll and phaeopigments. Two hundred and fifty milliliter samples were. filtered onto Whatman GF/F filters and processed for chlorophyll and phaeopigments following the method of Strickland and Parsons [13].

For the two months preceding the overflight, a physical and bio-optical mooring was placed near the. location of the outfall (Figure 1) by the. University of Southern California, Ocean Physics Group, with four instrument packages at depths from 10 m to 50 m in the water column. Each instrument package includes sensors for measuring temperature, conductivity, dissolved oxygen, orthogonal components of current, chlorophyll (Sea Tech fluorometer) and beam transmission at 660 nm (Sea Tech transmissometer). All data were recorded once per minute. The mooring was recovered two days before the. OVCI flight and sampling cruises, and the.re.fore was not contemporaneous with the overflight. 1 lowever, selected data are included because recent current history can have an important effect on the optical properties of the water column in this region.

Additionally, shipboard weather data and archived meteorological data were obtained from several sources for parameterizat ion of the atmospheric comet ion to the images.

4. Image calibration and atmospheric correction

in each spectral channel AVIRIS measures the following sum of radiances:

$$L_{tot} = L_w t_d(\theta_1) + L_{path} + L_{sky}*(\rho t_d(\theta_1) + \rho t_d(\theta_2)), \quad (1)$$

where:
L_{tot} = Total radiance, received at the aircraft (the, AVIRIS data)
L_w = wate,r-leaving radiance
$t_d(\theta_1)$ = diffuse transmission of the atmosphere at the instrument view angle
$t_d(\theta_2)$ = diffuse transmission at the solar zenith angle
L_{path} = path-scattered Rayleigh and aerosol radiance due, to the atmosphere
L_{sky} = skylight as viewed looking up from the surface., at the. instrument view angle
ρ = Fresnel reflectance of the water surface

Each of the terms on the right side. of the equation, with the exception of water-leaving radiance, was modeled with the atmospheric radiative transfer code LOWTRAN-7[14], A modified version of the model was used which allows a variable input for atmospheric watt.r vapor. This value is determined from the. uncorrected scene itself, by measuring the depth of the water absorption feature at 1130 nm. The intensity

of this absorption is proportional to the column abundance of water, and a scaling term was derived for the image. This is the continuum interpolated band ratio (CIBR) method of Bruegge[15] and Carrere[16], however no ground-truth sun-photometer measurements were available at the time of the. overflight. The modeling of column water abundance was therefore done. entirely with LOWTRAN-7, by applying a scaling factor to the amount of precipitable water predicted for the White Point scene (?..356 cm).

The exact column ozone abundance, was calculated for the date. of the overflight using current ozone profiles provided by the UARS (Upper Atmosphere Research Satellite) project. As the gas profiles used by LOWTRAN-7 are based on 1976 measurements, [O3] was rescaled for the atmospheric correction.

The model was run in radiance mode with the proper geometry and environmental characteristics to get the path-scattered term. It was run again with the observer placed on the surface looking up into space to get a value for skylight, which is then reflected off the ocean using the Fresnel reflectance (p) and diffusely transmitted through the atmosphere to altitude,.

Rearranging:

$$L_w(\text{image}) = [L_{tot} - L_{path} - L_{sky}^{*} (\rho t_d(\theta_1) + \rho t_d(\theta_2))]/t_d(\theta_1). \qquad (?)$$

The watcl-leaving, radiance thus derived from the image was then compared to in-situ measurements, collected by both in-water (MER1048) and surface (Spectron handheld spectroradiometer) instruments at station 2. The remote-sensing reflectance measurements taken with the Spectron were transformed to units of watm-leaving radiance, using a surface irradiance spectrum (E_d^{-}) calculated for the scene conditions using LOWTRAN-7:

$$L_w(\text{Spectron}) = R_{rs}^{*}E_d^{-}. \qquad (3)$$

The uppermost 5m of the underwater light field measurements were propagated to just below the surface using a polynomial interpolation, and then transformed to just above the surface using a factor of 0.544[12]:

$$L_w(\text{MER}) \approx L_u^{-}*0.544. \qquad (4)$$

The independent estimates of L_w are shown in figure 2. Agreement between the. various measurements is remarkably good, except in the short wavelengths. This is assumed to be an instrument calibration problem which is the. result of a change in instrument performance between conditions in the laboratory where it is calibrated and conditions in the aircraft (Rob Green, personal communication). Carder et al.[9] developed a vicarious recalibration technique which we employ here. We used the Spectron data for the recalibration and for this purpose, the higher spectral resolution measurements of the Spectron instrument were resampled to AVIRIS spectral channel positions and halfwidths. The ratio of the Spectron water-leaving radiance to the AVIRIS water-leaving radiance were them used to adjust the image calibration coefficients, and these new coefficients were applied to the entire image., This was performed only in the spectral region where the image calibration is unsatisfactory for a water target, i.e. for wavelengths less than 500 nm (the first 10 AVIRIS channels). 'l'his combination of modeling and vicarious recalibration (where necessary) was used to produce an atmospherically corrected and accurate. image for analysis.

5. Analyses and Discussion

Distinct water types were identified in the image and representative spectra (figure, 3) were extracted for analysis. Wind and wave eroded beach sediments can be seen extending from land (figure 1), and arc

characterized by high reflectance in the range 500-700 nm (figure 3). This is assumed to be sand, which are relatively large particles which rapidly settle out of the. surface water. These highly reflective plumes extend onl y a short di stance from shore and then end abruptl y, supporting the idea that they arc composed of large particles with a high settling rate.

A larger more diffuse plume extends from the outfall area to nearly the edge of the image. The wavelength of maximum reflected radiance in this area is identical to that of the beach sand (figure 3), however the magnitude is reduced by nearly a factor of 4. This plume is either from the outfall or the result of high current shear acting on the sediments along the slope-bmak, The final two days of mooring measurements of current speed and beam attenuation help to shed some light on this question (figure 4). These data were. collected with the. uppermost (1 O m) instrument package and support the idea that it is sediment resuspension. A significant increase in beam attenuation was recorded towar d the. end of the moor ing deployment (2 days prior to the overflight) and it was coincident with an increase in current speed associated with the storm (figure 4). We are uncertain as to the composition of these. particulates, however, these particles arc probably smaller in size since the. stayed suspended over a large area, and are probabl y composed of outfall effluent mixed with terr igenous silt.

A water-leaving radiance spectrum obtained from the AVIRIS image in an area with submerged kelp beds clearl y shows the chlorophyll "ml-edge." at 700 nm (Figure 3). Kelp require cool, clear nut rient-rich water and human activities which alter those conditions will reduce the extent of kelp beds. Remote-sensing kelp surveys have been proposed by Jensen and Estes[17] and in the region of an ocean outfall the. extent of kel p beds could be an important indicator of the ecological health of the area. The spectra of kelp reported by Jensen and Estes[17], and kelp spectra that we collected from Monterey Bay, do not have the high reflectance feature centered near 550 nm which is seen in the kelp spectra in Figure 3. Given the high level of suspended sediments in the surrounding watt.~ with a peak reflectance at 570 nm it is likely that suspended sediments in the kelp bed are contributing this signal. This was probably a temporary condition as the. result of the storm, however, if it were. to persist it would likely damage the. kelp.

The profile of percent transmission at station 2 (figure 5) shows reduced transparency in the surface waters due to an abundance of particles in the, top 25 m. The corresponding profile of chloroph yll fluorescence is low at the surface and peaks bet wccn 10 and 25 m, with a sharp decline to very low levels by 35 m. The temperature and salinity probes were not wor king when these measurements were collected, but the position of the chlorophyll fluorescence maximum indicates that a well-defined thermocline existed near 30 m, despite recent wind-mixing, Extracted chlorophyll values were. high throughout the top 20 m and actually highest at the surface (table 1). This change in fluorescence per unit chlorophyll is commonly observe.d (e.g. [18]) and is mused by light inhibition of phytoplankton fluorescence in the surface waters. Taking fluorescence inhibition into account the chlorophyll and percent transmission profiles are very similar indicating an abundance of particles, including phytoplankton mixed throughout the upper ?5 m.

Spectra from the three stations occupied for optical profiling are shown in figure 6. Station 3, furthest from shore, had nearly double the concentr at ion of chloroph yll and associated pigments of inshore station 2. (table 1). Its spectrum is clearly dominated by high absorption by phytoplankton pigments, without suspended sediments to elevate the signal near 500 nm. The position of peak water--lcavin~ radiance. is 550 nm, in contrast to the inshore stations, which peak at 500 nm.

Spectra from stations 1 and 2 appear quite similar, except in the short wavelengths (<480 rim). The station 1 spectr um has a strong absorption feature at 4S0 nm, indicating the presence of photosynthetic pigment, Station 2, however, shows much stronger absorpt ion in the shortest wavelengths measured, and lacks the clear absorption feature, at 450 nm. This suggests that the station 2 spectrum is highl y influenced by colored dissolved organic matter (CDOM), possibly from the sewage effluent.

All 3 station spectra show a slightly elevated signal near 683 nm indicative of solar induced chlorophyll fluorescence; in the. case of the inshore. spectra it is superimposed on the elevated sediment signal. The fluorescence signal is clearest in the spectra from station 3 which correlates with higher chlorophyll (table 1) at that station and the 683 fluorescence signal observed in the BOPS data (not shown). Solar-induced fluorescence of chlorophyll has been mapped at low altitude with a prototype airci aft imaging spectrometer[19]. in waters with high chlorophyll (> 2 mg/m^3) the, 683 nm fluorescence, signal may be the best tool for estimating phytoplankton abundance as it is relatively free of interference from the. signals from suspended sediments or dissolved organics which are often high in coastal productive. waters.

'1'here was a large swell at the time of the. overflight and in the northeast corner of the image it was rotated so that it was oriented towards and away from the sun. The side of the. swell towards the sun was significantly brighter duc to surface reflected sunlight. An area of the image where this pattern was particularly obvious was selected to determine how this patter-n affects the signal of an ocean color instrument with a spatial resolution that would be unable to resolve this difference. Light and dark pixels within this area were separated, and their spectra are shown in figure 7, along with the difference bet ween the two. Approximatel y 20% of the pixels in the area chosen for this analysis (1 square. km) were affected by this directly reflected beam. The radiance. offset has slight spectral structure., and is highest at 550 nm generally reflecting the shape of the solar spectrum. Using the mean of the light and dark samples as representative of a spatially integrated signal the potential error from including the bright pixels was calculated. The error has a spectral shape and is largest where the actual signal is smallest (figure 7). This could produce a significant error in data products from moder atc r esolution inst ruments which average. over 1 square km and use band-ratio algor ithms.

Previousl y published algorithms were used to estimate the inherent optical proper tics of the area. Assuming that absorption at 660 nm is primarily from water and adding a slight correction for the phytoplankton wc calculated backscatter at 660 nm from the remote sensing reflectance at that wavelength. Figure 8 shows b_b and R_{rs} along a transect from the clearer water offshore into the nearshore high sediment plume.. Consistent with the work of Carder et al .8, wc find a greater separat ion of b_b and R_{rs} as reflectance of the scene increases. However for our data there is a 12.X difference in the magnitude of these, estimates while Carder et al.[8] found a ratio of 3.35. Clearly, these relationships arc regional, and most likely dependent on the composition of the suspended particles. An image of backscatter at 660 nm was created (figure 9). It clearly shows the high sediment plumes coming off the beaches and the moderate sediment levels in the middle of the image associated with either the outfall or shelf break sediment resuspension.

6. Summary and Conclusions

An imager with a few discrete channels will not provide adequate information to separate the chlorophyll signal from the signal from dissolved organics, detritus, suspended sediments, bottom reflectance, kelp and other features that arc often found in the coastal zone. As one approach to overcome these problems we have been working with AVIRIS to test the utility of imaging spectrometer data for studies in coastal waters, To date wc have demonstrated the ability to separate the chlorophyll signal from bottom reflectance in clear waters of 1 .ake Tahoe[12] and the. turbid waters offshore from Tampa Bay[9]. in addition signals from re- suspended sediments anti di ssolved organics have been interpreted for Tampa AVIRIS images[8,9]. Here we examined differences in spectra from different areas of an AVIRIS image of San Pedro Channel. Spectral signals from large particles of beach sand and either resuspended bottom material or effluent from the outfall show sufficient difference to allow separation. Near-shore, kelp beds are identifiable from their spectral signature, even with a sediment signal superimposed, The spectra from the sampling stations were examined, arid show differences between one another that arc related to the suspended sediment nearshore, and high chlorophyll offshore. Both near- and offshore spectra show the effect of CDOM.

A part of the image which showed the effect of specular reflectance was examined in detail. The offset between glinted and unglinted pixels had a spectra similar to sunlight, with a magnitude of as much as 0.4 $mW\ cm^{-2}\ sr^{-1}\ nm^{-1}$ at 550 nm. Approximately 20% of the pixels in the, test area were contaminated with this direct reflectance, and this effect could significantly bias estimates of chlorophyll concentration made. with moderate resolution imagers which integrate over much larger spatial scales.

An algorithm for estimating backscatter from an AVIRIS image that was developed for Tampa Bay was applied to this image. The ratio of b_b to R_{rs} was very diffc.rent for San Pedro Channel compared to Tampa Bay and this highlights the. need for regional algorithms for case 2 waters.

7. Acknowledgments

In situ measurements were made from the R/V Sea Watch and we thank the Captain and crew for their assistance with this effort. We thank the JPL AVIRIS team and the NASA Ames Research Center, High Altitude Branch for collecting the AVIRIS data. Thanks to William Read for the UARS ozone data and to Tom Dickey, Department of Geosciences, University of Southern California for providing the mooring, data.

"l'his work was carried out at the Jet Propulsion 1 aboratory, (California Institute of Technology and the University of South Florida, and was supported by contracts from the National Aeronautics and Space Administration to those institutions. References herein to any specific commercial product, process, or service by trade name, trademark, manufacturer, or otherwise, dots not constitute or imply its endorsement by the United States Government, the Jet Propulsion Laboratory, (California Institute, of Technology or the University of South Florida.

8. References

1. J. R. 1 lerring, "Wastewater particle dispersion in the southern California offshore region," Particulates in Water: Characterization, Fate and Removal, M. C. I eckie and J. O. I eckie, eds., American Chemical Society, Washington D. C., pp. 2.83-304, 1980.
2. Y. Wu, 1.. Washburn and B. }1. Jones, "Buoyant plume dispersion in a coastal envrionment: Evolving plume structure and dynamics," *Continental Shelf Res.*, InPress.
3. 11.11. Jones, A. Bradkovich, T. Dickey, G. Kleppel, A. Steele, R. Iturriaga, and I. Haydock, "Variability of physical, chemical and biological parameters in the vicinity of an ocean outfall plume," Startified Flows: Proceedings of the Third International Conference on Stratified Flows, E. J. List and G. H. Jirka, eds, ASCE, Ncw York, pp. 877-890, 1990.
4. 1.. Washburn, B. Jones, A. Bratkovich, '1'. Dickey, and M. Chen, "Mixing, Dispersion, and Resuspension in Vicinity of Ocean Wastewater Plume," *Journal of Hydraulic Engineering*, 118(1), 38-58, 1992.
5. S. B. I looker, et al., SeaWiFS Technical Report Series, Volume 1, An overview of SeaWiFS and Ocean Color, NASA Tech. Memo. 104566, Vol. 1, 25 pp.
6. A, Morel and 1.. Prieur, "Analysis of variations in ocean color," *Limnol. Oceanogr.* 22(4): 709-722, 1977.
7. W. M. Porter, and H. "l'. Enmark, "S ystem overview of the Airborne Visible/lr~frarcd imaging Spectrometer (A VI RIS)," Proc. SPIE 834, Imaging Spectroscopy II, Int. Soc. Optical Eng., Bellingham, WA, pp. 114-126, 1987.
8. K.L. Carder, R. Steward, R. Chen, S. Hawes, Z. Lee, and C. Davis (1993), AVIRIS calibration and application in coastal environments: tracers of soluble and particulate constituents of the Tampa Bay coastal plume, *Photogrammetric Engineering and Remote Sensing*, 59(3), pp. 339-344.
9. K.]. Carder, P. Reinersman, R. Chen, F. Muller-Karger, C. O. Davis and M. K. Hamilton, "AVI RIS calibration and Application in Coastal Oceanic Environments", *Remote Sensing of Environment*, 44:, in press.

10. S. H. Pilorz, and C. O. Davis, "investigations of ocean reflectance with AIVIRS data," Proceedings of the Second Airborne Visible/Infrared Imaging Spectrometer Workshop, JPL Publication *90-54, pp.* ?24-?31 , 1990.
11.1-1. C. Smith, C. R. Booth, and J, 1.. Stat, "oceanographic Bio-optical Profiling S ystem," *Applied Optics, 2.?,* 2.791 -2s797, 1984.
12. M, K. Hamilton, C. O. Davis, W, J, Rhea, S. H. Pilorz and K, L. Carder, "Estimating chlorophyll content and bathymetry of Lake Tahoe using AVIRIS data," *Remote Sensing of the Environment*, 44: In Press.
13. J. D. H. Strickland and '1'. R. Parsons, A Practical Handbook of Seawater Analysis, Fish. Res. Bd. Canada Bull. 167, 311 pp., 1972..
14. F. X. Kneizys, E. P. Shettle, 1.. W, Abreu, J. H. Chetwood, G. P. Anderson, W. O. Galler y, J. E. A. Selby, S. A. Clough, "Users Guide to LOWTRAN 7," Air Force Geophysical 1 aboratory, AFGL-TR- 88-0177, *Environmental Research Papers, No. 1010,* 1988.
15. C.J. Bruegge, J.E. Conel, J.S. Margolis, R.O. Green, G. Toon, V.E. Carrere, R.G. Holm, G. Hoover, "in-Situ Atmospheric Water-Vapor Retrieval in Support of AVIRIS Validation, " in Imaging Spectroscopy of the Terrestrial Environment, G. Vane, ed, Proc. SPIE 1298, Orlando, Florida, pp. **150-163, 1990,**
16. V, Carrere, J. Conel, R. Green, C. Bruegge, J. Margolis, and R. Alley, "Analysis of Atmospheric Water Vapor Maps from AVIRIS at Salton Sea, California: Part I, Experiments, Methods, Results, and Error Budgets, " in Proceedings of the Second AVIRIS Workshop, R. Green, ed., JP1. 90-54, 107-128, 1990.
17. J. R. Jensen, J. E. Estes, and M. Mel, "Multispectral kelp resource survey s," Satellite Hydrology, American Water Resources Assoc., pp. *533- 542., 1979,*
18. J. J. Cullen, M, R. Lewis, C. O. Davis and R. '1'. Barber, "Photosynthetic Characteristics and Estimated Growth Rates Indicate Grazing Is the Proximate Control of Primary Production in the Equatorial Pacific," *J. Geophys. Res. 97(C1): 639-654, 1992.*
19. J. F. R. Gower, and G. A, Borstad, "Mapping of phytoplankton by solar-stimulated fluorescence using an imaging spectrometer," *Int. J. Remote Sensing,* 11: 313-320, 1990.

'l'able 1. Extracted chlorophyll and phaeopigment values (mg/l) from water collected at stations 2 and 3.

Station 2.. time 1315 PST. 33°40.93' N, 118°18.29' W

sample	depth (m)	chlorophyll	pheaopigments	chl+ phaeo
1	2	1.2.8	0.6S	1.93
2.	10	**0.90**	**0.53**	**1.43**
3	20	**0.95**	**0.51**	1.46
4	40	**0.10**	**0.35**	**0.45**

Station 3. time 1415 PST. 33°36,12' N, 118°21 .32'W

sample	depth (m)	chlorophyll	pheaopigments	chl+ phaeo
5	2	2.15	**0.80**	2..95
6	10	1.63	0.82.	2..45
7	20	2.37	**0 . 9 0**	**3.27**
8	**40**	**0.60**	**0.56**	**1.16**

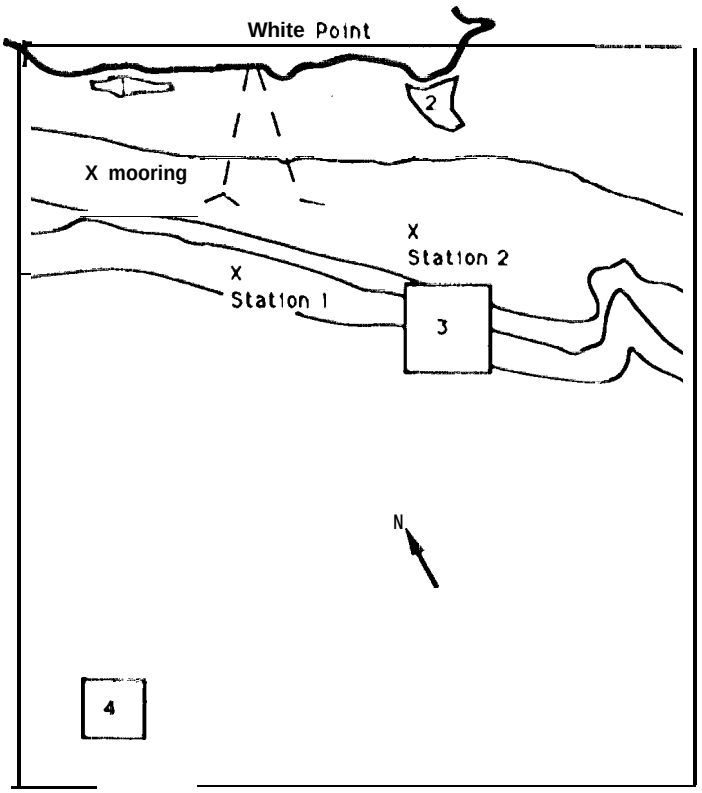

1. Location map of the White Point/San Pedro Channel study area. The box indicates the extent of the AVIRIS image. Spectra were analyzed from sampling stations and from four representative areas; 1) kelp beds, 2) beach erosion sediment plume, 3) diffuse plume near the outfall, and 4) 'dark water' - a region outside the plume which had the lowest reflectance in the image.

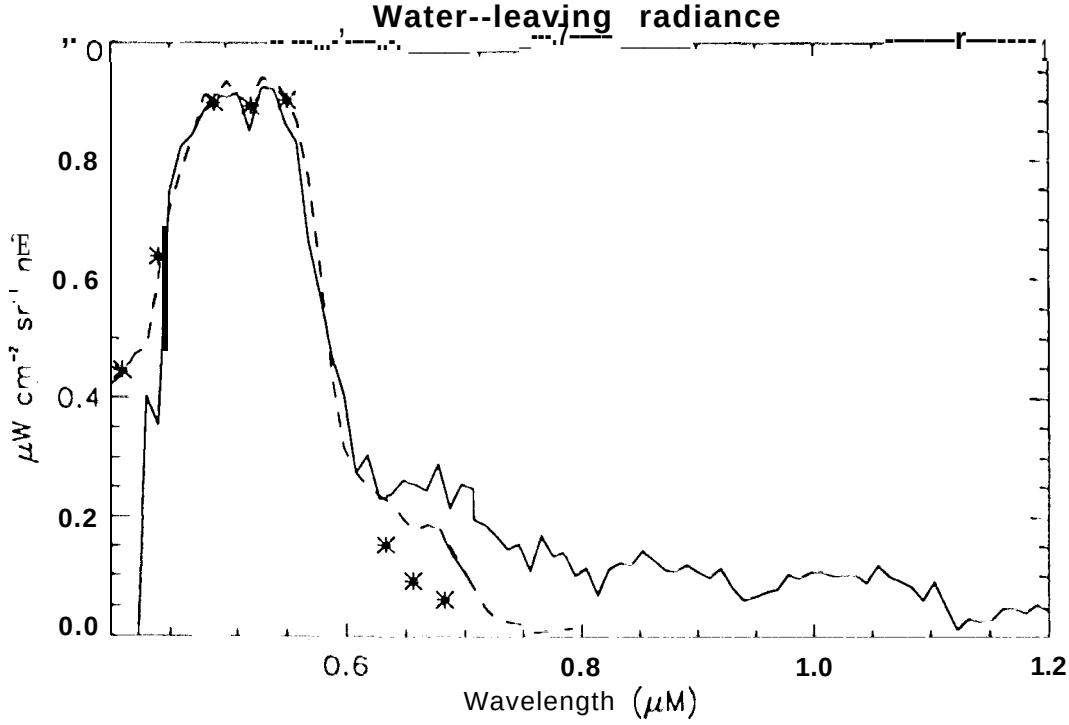

2, Water-leaving radiance as estimated by in-water measurements (asterisks), R_{rs} (dashed line), and the AVIRIS image (solid line).

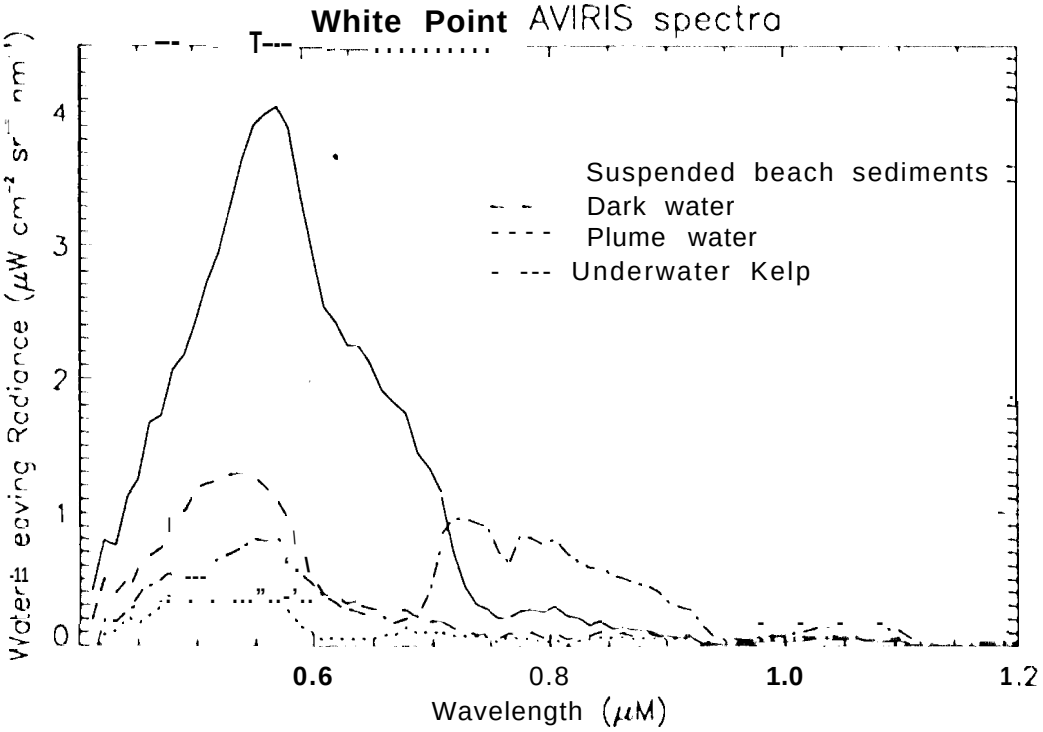

3. Mean spectra extracted from four distinct areas in the AVIRIS image as indicated in figure 1. The signal-to-noise ratio was enhanced at least S fold by averaging.

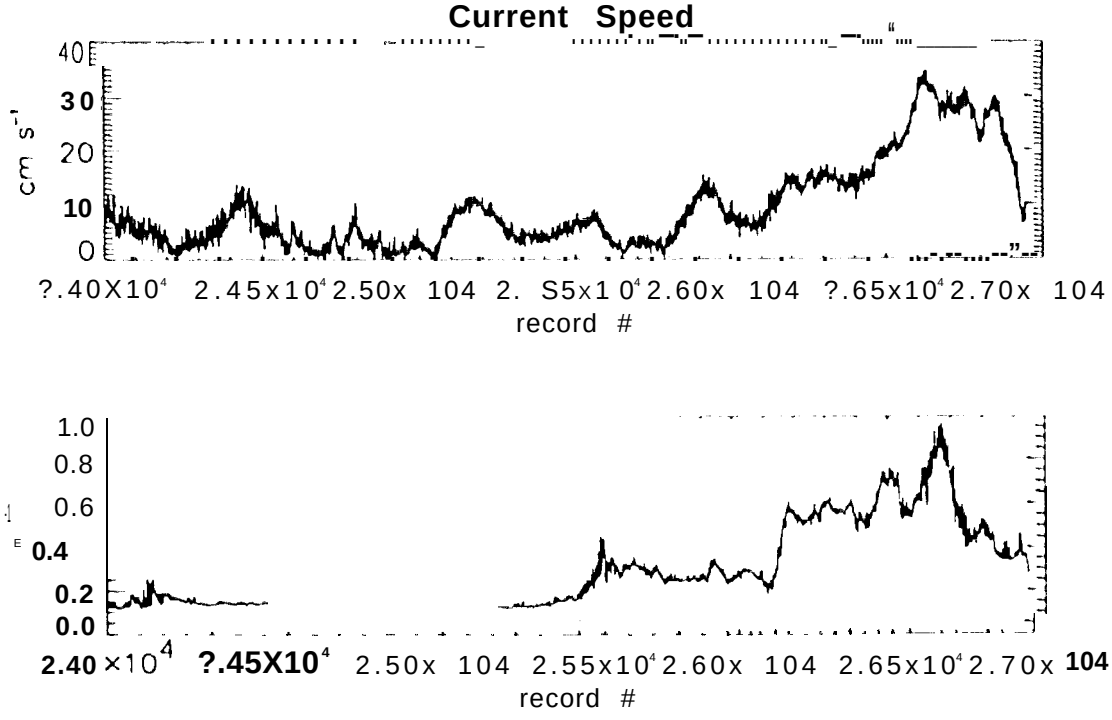

4. Current speed and beam attenuation coefficient (with the attenuation of water removed) measured during the last two days of the mooring deployment. The abscissa is record number, and records were collected once per minute. The predominant current direction w'as along the coast towards the northeast.

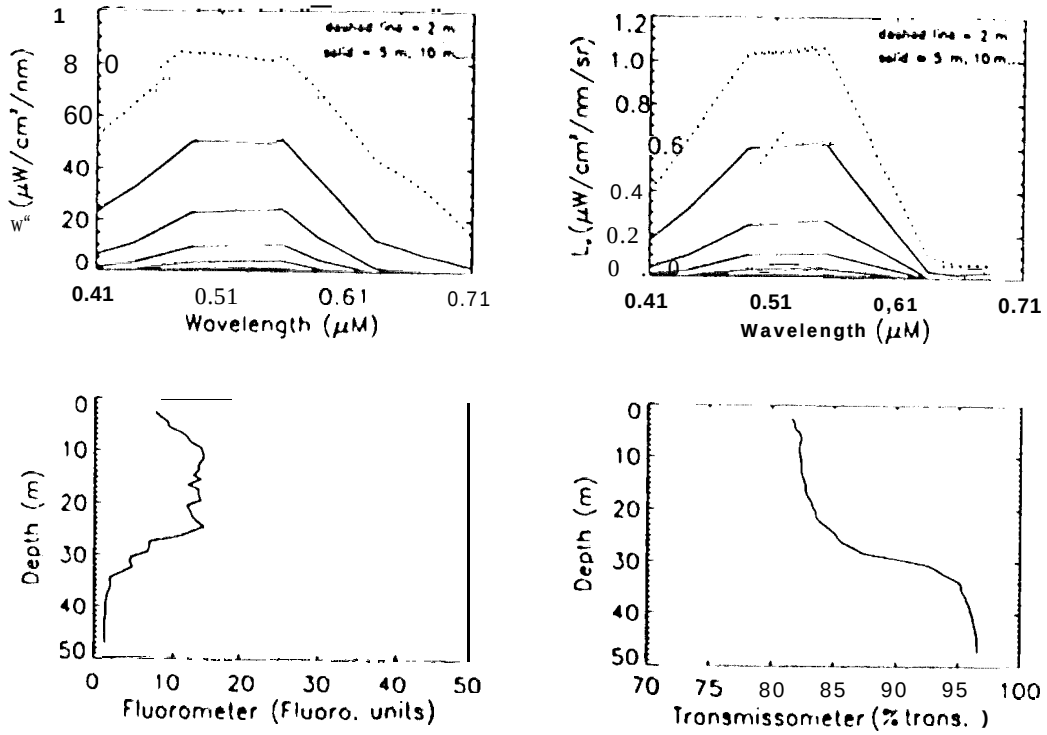

5. Spectra of the underwater light field at various depths at station 2, and profiles of chlorophyll fluorescence and percent transmission of collimated (660 nm) light,

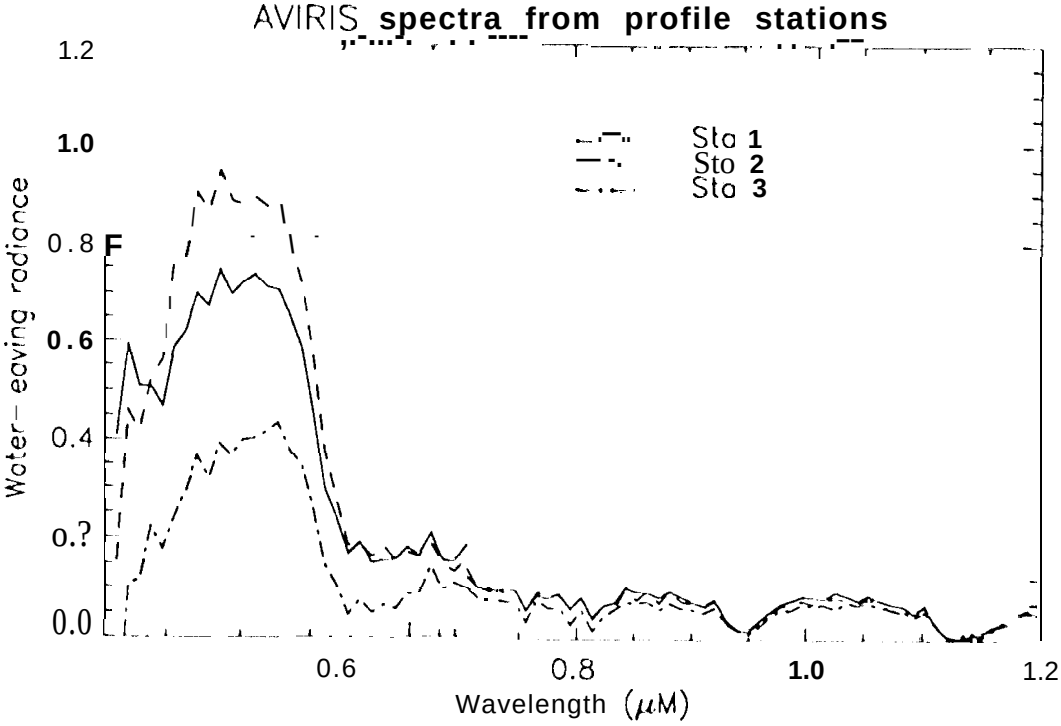

6. Spectra extracted from the AVIRIS image, at the profiling stations occupied on 21 March, 1991. Each spectrum is a mean from a 50X 50 pixel area.

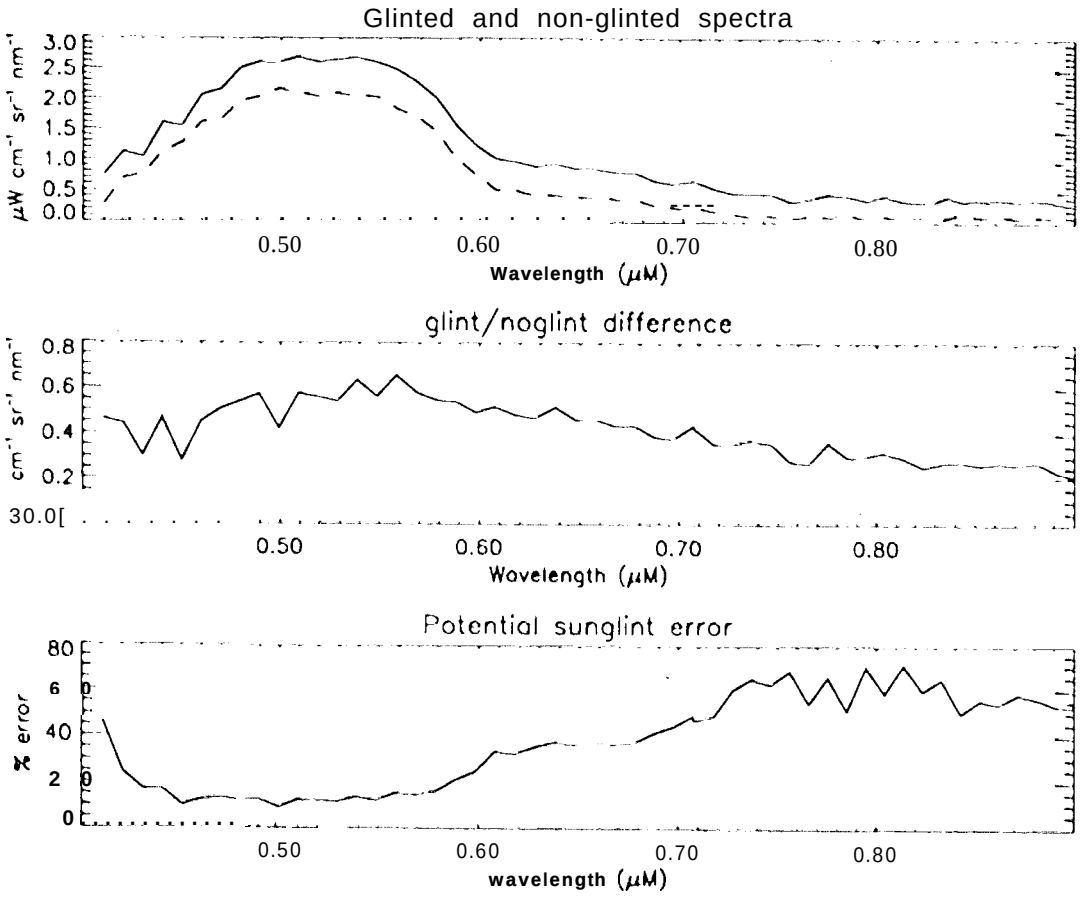

7. Spectra extracted from the AVIRIS image, in a region of specular reflectance showing the magnitude of the enhanced signal and the potential error in retrieved radiances.

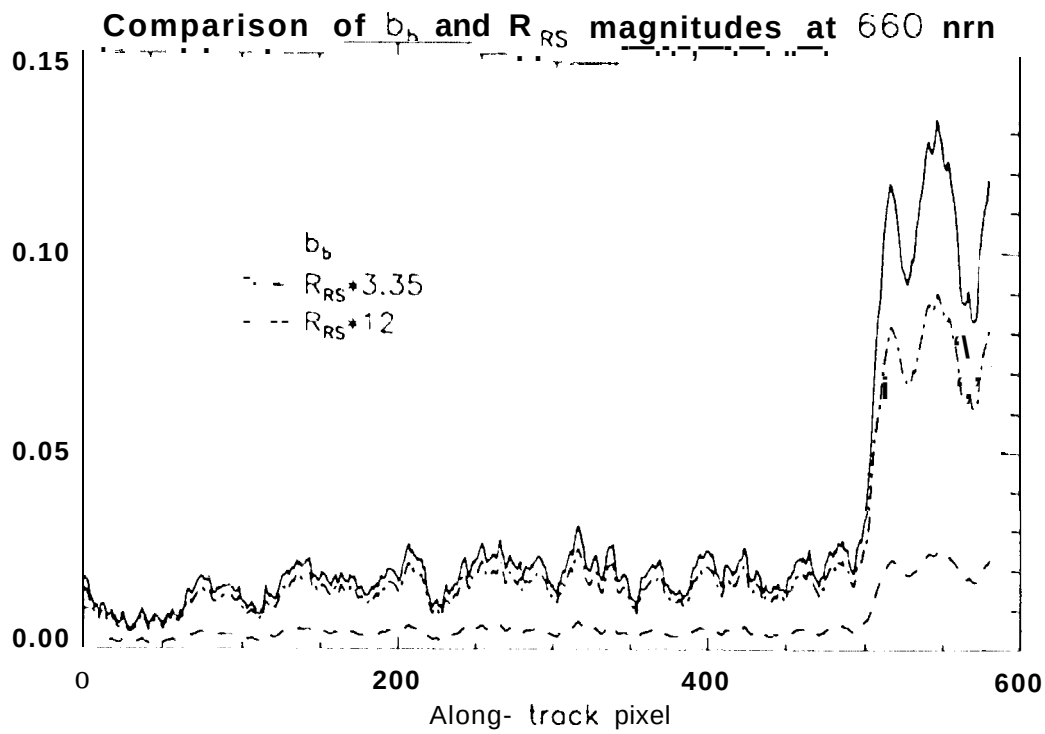

8. Comparison of Rrs (660 nm) and b_b (660 nm), each derived from the AVIRIS image. Separation between the two increases with increasing reflectance of the scene, and the offset between the two is nominally a factor of 12.

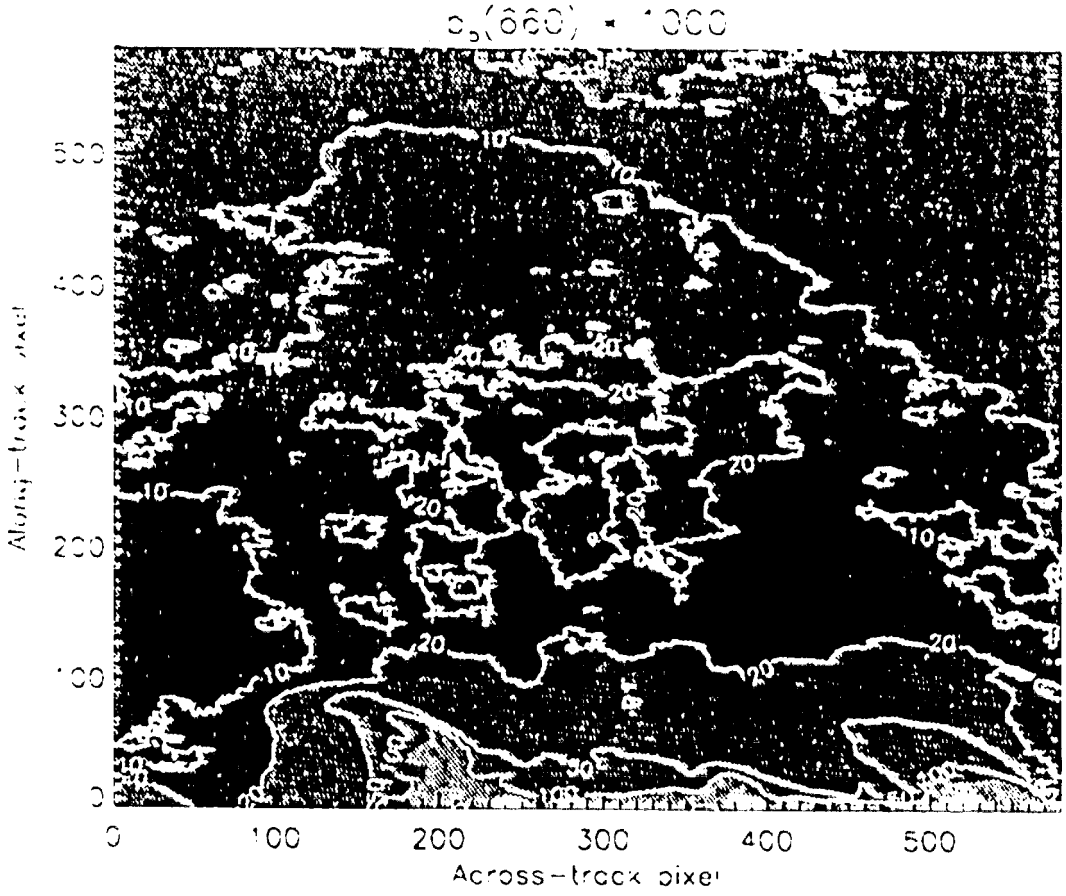

9. *The* contoured image of **backscattering** coefficient at 660 **nm.** Values have been multiplied by 1000 for clarity.